Measuring Crystal Size in Cirrus Using 35 and 94 GHz Radars

ROBIN J. HOGAN*, ANTHONY J. ILLINGWORTH AND HENRI SAUVAGEOT†

Department of Meteorology, University of Reading, UK

†*Université Paul Sabatier, Toulouse, France*

J. Atmos. Oceanic Tech., 2000, **17**, 27–37

ABSTRACT

Results are presented from a case study in which coincident 35 and 94 GHz radars located at Chilbolton, England, were used to measure crystal size in cirrus. In the presence of larger crystals the 94 GHz radar scatters sufficiently beyond the Rayleigh regime that the difference in reflectivity factor measured by the two can be directly related to size. This enables more accurate estimation of ice water content than would be possible using a single radar. The small crystals at the top of the cloud scatter in the Rayleigh regime at both wavelengths, which provides a valuable method of calibration, but also means that sizing is not possible in this part of the cloud. Ice water content and median volume diameter were derived and compared with the analyses of the UK Meteorological Office Unified Model. The smallest measurable median volume diameter in this case study was around 200 μm, although it is believed that with both radars sensitive down to -35 dBZ, it should be possible to measure median diameters of 100 μm. Scattering calculations have been carried out to determine the sensitivity of these measurements to crystal density, crystal aspect ratio and the shape of the size distribution. Density is found to be the most significant source of uncertainty, possibly introducing errors of 20% into retrieved diameter.

1. Introduction

Cirrus clouds represent an important but challenging problem in the understanding of the climate system (Stephens et al. 1990). Measurements of ice water content (IWC), effective radius (r_e) and optical depth are required to determine their effect on the earth's radiation budget and to validate climate models. Currently such models tend to carry cloud water content as a prognostic variable and relate this to radiative properties by means of an effective radius which is usually fixed; for example, the UK Meteorological Office (UKMO) Unified Model prescribes a value of 30 μm (Martin et al. 1994). There is a need to test the skill of models to diagnose IWC, and to determine whether a fixed value of r_e is adequate. A global climatology of cirrus would be particularly useful, although this could only be obtained from a satellite-borne radar or lidar.

It is generally accepted that cirrus clouds cause a net warming of the climate system, but exact calculation of their radiative properties is very difficult because of the multitude of crystal habits that are present. This introduces uncertainty into the interpretation of remotely sensed measurements, and to simplify matters it is common to assume, for the purposes of solar, infrared and millimeter-wave radiative transfer calculations, that ice crystals can be adequately represented by spheres or spheroids. Aspect ratio and crystal density remain free parameters and must be prescribed in remote retrieval algorithms if they cannot be measured directly.

**Corresponding author address:* Department of Meteorology, PO Box 243, Earley Gate, Reading RG6 6BB, UK. E-mail: r.j.hogan@reading.ac.uk.

It was shown by Brown et al. (1995) using measurements of crystal size spectra by aircraft that radar reflectivity factor (Z) from a 94 GHz radar can be used to estimate IWC to an accuracy of +100% and -50% (3 dB), but that if additional information regarding crystal size is present then this error can be reduced to less than +40% and -30% (1.4 dB). Several techniques have been proposed to retrieve vertically-resolved estimates of crystal size. Matrosov et al. (1994) used a vertically-pointing Doppler radar to measure crystal fall velocity, from which size was estimated using an empirical relationship. Intrieri et al. (1993) demonstrated the use of combined radar and infrared-lidar measurements to infer size. However lidars are subject to significant attenuation in moderately thick cirrus, and furthermore a large fraction of mid-latitude cirrus occurs in conjunction with liquid-phase clouds at lower levels which can completely extinguish the signal from a ground-based instrument.

Two radars at different wavelengths have the capability to estimate hydrometeor size, because, as diameter increases, the shorter wavelength scatters in the Mie rather than the Rayleigh regime and its reflectivity falls below that at the longer wavelength. This principle was first proposed by Atlas and Ludlam (1961) as a means of hail detection using, for instance, a Rayleigh-scattering S-band radar together with an X-band radar that Mie-scatters only in the presence of large hail. Such schemes have always had to contend with differences in reflectivity due to attenuation by rain at the shorter wavelength (Tuttle and Rinehart 1983), and it was found that even with well matched beams of very similar beamwidth, differences in the sidelobe level were able to cause large reflectivity differences in the vicinity of strongly reflective cores where a signifi-

cant fraction of the signal is returned from the side-lobes (Rinehart and Tuttle 1982). However, it was the ambiguity caused by the very different scattering properties of wet and dry hail that made this technique unworkable.

In this paper we use 35 and 94 GHz radars, and at these frequencies dual-wavelength observations of cirrus suffer none of these problems; attenuation by ice is generally small enough to be neglected, attenuation by atmospheric gases is a minor correction, and reflectivity gradients comparable in magnitude to those at the edge of the cores of convective storms are never observed. Attenuation by supercooled liquid water in mixed-phase clouds could in theory cause the technique to produce erroneous results. However the cirrus observed in this case study had a temperature ranging between -50 and -20°C, and previous observations of liquid water clouds at temperatures below -10°C have all shown them to have water contents of less than 0.1 g m^{-3} (e.g. Herman and Curry 1984; Sassen 1991; Heymsfield et al. 1991). At -20°C this corresponds to a differential attenuation of only 0.4 dB km^{-1}, so this effect is typically much smaller than differences in reflectivity due to Mie scattering.

The dual-wavelength ratio, defined simply as

$$\mathrm{DWR} = 10 \log_{10} \left(\frac{Z_{35}}{Z_{94}} \right) \ \mathrm{dB}, \qquad (1)$$

is directly related to some measure of average crystal size, where Z_{35} and Z_{94} are the reflectivity factors (in mm^6 m^{-3}) measured at 35 and 94 GHz respectively. The use of dual-wavelength radar for sizing in cirrus was first proposed by Matrosov (1993) who carried out scattering calculations for a first-order gamma distribution of solid-ice spheroids with a variety of different wavelength combinations and aspect ratios. In each case DWR was calculated as a function of D_0, the median diameter of the volume-weighted size distribution. Recently, Sekelsky et al. (1999) used three colocated radars at 2.8, 33 and 95 GHz to estimate crystal size in precipitating and non-precipitating ice clouds. Size was derived from the measurements using a neural network trained with the results of theoretical scattering calculations also using a first-order gamma distribution of crystals. Here we follow the approach of Hogan and Illingworth (1999) and use real size spectra measured by the UKMO C-130 aircraft during the European Cloud Radiation Experiment (EUCREX) to determine the best relationship between DWR and D_0. At large crystal sizes this is found to differ appreciably from those calculated using idealized analytic expressions for the size distribution.

There is an intrinsic lower limit to the size that can be measured by this method, which is reached when the random error in DWR at low signal-to-noise ratio is of the same order as the magnitude of DWR due to Mie scattering. The use of higher frequencies such as 140 or 215 GHz would enable smaller sizes to be measured, for the simple reason that DWR would be considerably larger for a given D_0; Hogan and Illingworth (1999) investigated the potential of a spaceborne dual-wavelength radar to make global measurements of crystal size in cirrus, and showed that the most promising frequency combination was 79 (or 94) and 215 GHz, being in general more accurate than the combination of 35 and 94 GHz. However, attenuation by liquid water and water vapor in the lower troposphere is such that the use of frequencies much higher than 94 GHz to monitor cirrus clouds is unfortunately not feasible from the ground.

The next section describes scattering calculations that have been carried out to determine DWR as a function of D_0, and to investigate the sensitivity to variations in crystal density, crystal habit, and the shape of the size distribution. In Section 3 results are presented from a case study in which thick cirrus was observed at vertical incidence by the 35 and 94 GHz radars at Chilbolton, England. Microphysical parameters are derived and compared with those diagnosed by the Mesoscale Version of the UKMO Unified Model. In addition we investigate the evolution of microphysical properties in cloud parcels by tracing the variation of IWC and D_0 along individual fallstreaks.

2. Scattering calculations

In this section we examine theoretically the assumptions that are necessary to make quantitative deductions from dual-wavelength radar measurements. Scattering calculations have been carried out using the T-matrix method which is applicable for homogeneous spheroids (Waterman 1969). Calculations using more advanced methods to compare realistic shapes, such as hexagonal columns and plates (Schneider and Stephens 1995) and dendritic snowflakes (O'Brien and Goedecke 1988), with equivalent spheroids show that the errors associated with the spheroidal approximation are in general less than 15% (0.6 dB), provided maximum dimension, aspect ratio and total ice mass are maintained.

In the first instance we follow the experimental findings of Kosarev and Mazin (1989) and assume the size spectra of ice crystals are well approximated by the gamma distribution:

$$n(D) = N_0 D^{\mu} \exp\left(-\left[3.67 + \mu\right] D/D_0\right), \qquad (2)$$

where μ is the shape parameter and D is equivolumetric diameter. The validity of this assumption is examined later by comparing with real size spectra measured by aircraft.

We need to relate DWR to D_0 and to the parameter R_f, defined simply as reflectivity factor at frequency f

divided by IWC:

$$R_f(D_0) = \frac{Z_f}{\mathrm{IWC}}$$

$$= \frac{\int_0^{D_{\max}} \frac{|K(\rho)|^2}{0.93} D^{6+\mu} \exp(-3.67 + \mu D/D_0)\gamma_f(D)\, dD}{\frac{\pi}{6}\int_0^{D_{\max}} \rho D^{3+\mu} \exp(-3.67 + \mu D/D_0)\, dD} \quad (3)$$

where $\gamma_f(D)$ is the Mie/Rayleigh backscatter ratio. Hence an estimate of R_{35} from DWR can be used to obtain IWC simply from IWC $= Z_{35}/R_{35}$. Note that (2) is not normalized, but that the number concentration parameter N_0 has been cancelled from (3). However the density of the ice-air lattice ρ remains in (3) and must be prescribed as a function of D. The dielectric parameter $|K|^2$ has been calculated as a function of density using the expressions of Maxwell-Garnet (1904) and Liebe et al. (1989), and is almost identical at 35 and 94 GHz. It should also be noted that both $|K|^2$ and $\gamma_f(D)$ are virtually independent of temperature. The value 0.93 is present in (3) to make reflectivity factor relative to liquid water at centimeter wavelengths.

The ice crystal distributions given by (2) have been discretized into 500 sizes ranging from 10 μm to $D_{\max} =$ 5 mm in 10 μm intervals. In the following sensitivity studies, D_0 and R_{35} are plotted as functions of DWR for various values of μ, ρ and aspect ratio.

a. Sensitivity to density

An important consideration for cirrus retrievals is the density of the crystals. Brown and Francis (1995) examined data from aircraft flights through cirrus, and by comparing IWC estimates from the Total Water Probe and the 2D probes, were able to derive an empirical expression relating crystal mass to the mean of the maximum crystal dimensions in the directions parallel and perpendicular to 2D photodiode array. If one assumes that the crystals in this study were spherical (e.g. Brown et al. 1995), then for a diameter greater than around 100 μm, ice crystal density is given by

$$\rho = 0.07 D^{-1.1} \ \mathrm{g\,cm^{-3}} \quad (4)$$

where D is in millimeters. Below 100 μm the density of solid ice is adopted. However, Fig. 4 of Brown and Francis (1995) indicates that even with this density function, the IWCs derived using the two instruments differ with an RMS difference of around $\pm$40%. Although much of this disagreement may be attributable to instrumental error, the possibility remains that density may vary considerably from cloud to cloud. The effect of a 40% error in density is explored by considering the density functions $\rho = 0.05 D^{-1.1}$, and $\rho = 0.1 D^{-1.1}$ g cm^{-3} in addition to that given by (4).

The top row of Fig. 1 shows the variation of D_0 and R_{35} with DWR for these three densities, assuming an exponential size distribution ($\mu = 0$). Because DWR is independent of density for a single crystal, under- or overestimating the density of all crystals in the distribution by the same factor has *no effect* on the size derived from DWR. There is a direct effect on the derived IWC however (indicated by the value of R_{35}). Reflectivity factor is approximately proportional to ρ^2, so for a given measured Z and DWR, the inferred IWC is approximately inversely proportional to ρ. Note that single wavelength estimates of IWC are susceptible to random variations in density from cloud to cloud in exactly the same way, and the errors quoted by Brown et al. (1995) for the accuracy of such measurements took no account of this.

It would seem unlikely that the largest crystals, which may be growing by aggregation, should continue to decrease in density at the same rate. It is conceivable that if the crystals in the Brown and Francis (1995) study were distinctly non-spherical then (4) could be significantly in error. In fact Francis et al. (1998) derived a relationship between crystal mass and the cross-sectional area measured by the 2D probes using essentially the same data as Brown and Francis. However we found that when the spherical assumption is applied to this relationship, the density has the form

$$\rho = 0.175 D^{-0.66} \ \mathrm{g\,cm^{-3}}, \quad (5)$$

which is significantly larger than (4) for crystals with diameters of 300 μm and above. The difference stems from the fact that most of the crystals in the dataset were rather irregular. Consequently the 'equivalent-area diameter' that D represents in (5) is systematically smaller than the mean of the maximum dimensions that was used in (4), and hence the derived density is correspondingly larger. The question of which of the two definitions of diameter is closer to that which determines the extent of Mie scattering for a millimeter-wave radar still remains to be answered.

The bottom row of Fig. 1 shows the effect of density functions (4) and (5) on size and IWC retrievals. It can be seen that derived IWC differs by more than a factor of two, while size changes by no more than 20%. Clearly more work is required to resolve this issue, possibly involving reinterpretation of 2D probe data, but in this paper we shall use the density given by (4).

b. Sensitivity to crystal habit

Until now we have assumed that crystals can be approximated as spheres, but in reality they occur in a multitude of different shapes and tend to fall with their longest axis parallel to the ground (see Liou 1986, and references therein). This could prove to be a problem for vertically-pointing dual-wavelength radar, because the extent of the deviation of Z_{94} from the Rayleigh approximation is not

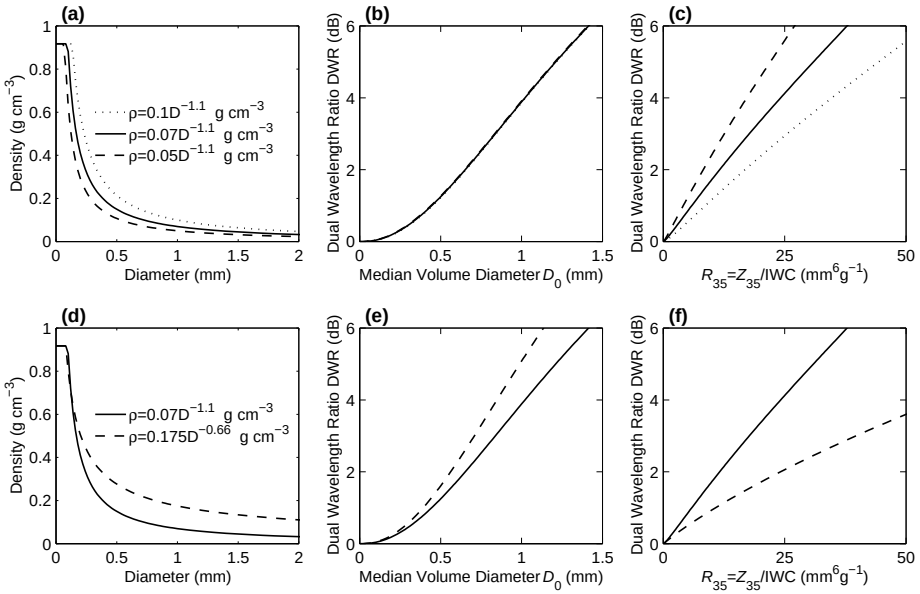

FIG. 1: The sensitivity of dual-wavelength retrieved quantities to density, for an exponential distribution of ice crystals. The density functions described in the text are plotted in (a) and (d), with DWR as a function of D_0 and R_{35} to their right.

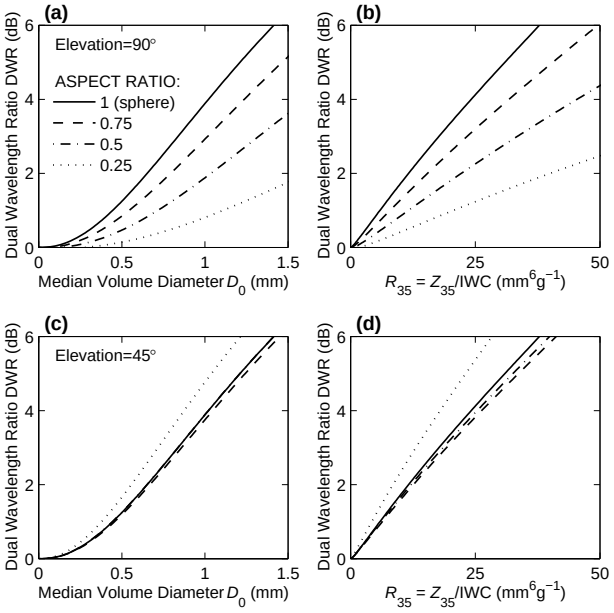

FIG. 2: DWR as a function of D_0 and R_{35} at vertical incidence (top row) and at an elevation of 45° (bottom row), for oblate crystals of four different aspect ratios. The radiation is vertically polarized at both wavelengths and the distribution is exponential.

so much a function of D_0, as of the dimension of the crystals in the direction parallel to the direction of propagation of the incident radiation. At vertical incidence this dimension is in fact the shortest axis of the crystal, so the effect of assuming that non-spherical crystals are spherical is to underestimate D_0. This is illustrated in the top row of Fig. 2, where it can be seen that oblate crystals with aspect ratios of 1, 0.75, 0.5 and 0.25 produce a large range of D_0 and R_{35}; for example the presence of crystals with an axial ratio of 0.5 results in D_0 being underestimated by a factor of two and IWC overestimated by a similar amount. Calculations for prolate crystals (not shown) produce similar results.

A straightforward solution to this problem is to dwell at an elevation of 45°, so that the dimension on which DWR depends is much closer to the equivalent spherical diameter. The bottom row of Fig. 2 shows that for observations at an elevation of 45° (using vertically-polarized radiation at both wavelengths), horizontally aligned crystals behave very much like spheres and the fact that aspect ratio is unknown is far less important. It is found that down to aspect ratios of around 0.4 the spread in retrieved parameters is less than ±5%, but the error reaches 25% for aspect ratios of 0.25. This is likely to also be the case both for canting crystals that are on average horizontally aligned, and for randomly oriented crystals. It is important however that DWR is calculated using the same polarization at both frequencies. In this study the radars were vertically-pointing, but in future the strategy of dwelling at 45° may be adopted.

c. Sensitivity to distribution shape

To test the sensitivity of retrieved parameters to the shape of the distribution, three values for the shape parameter μ (-1, 0, 2) were considered. The corresponding plots in Fig. 3 suggest that derived quantities should be fairly insensitive to the typical range of μ that one would

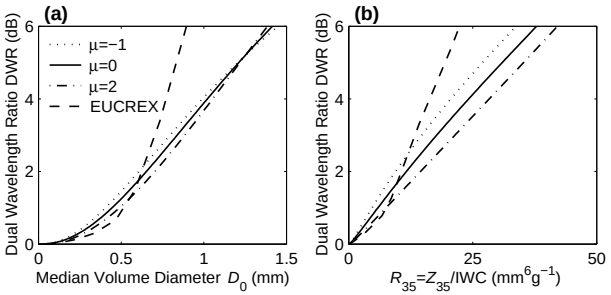

FIG. 3: DWR as a function of D_0 and R_{35} for gamma distributions with three values of the shape parameter μ, and as derived empirically from real size spectra measured during EUCREX.

expect in cirrus, varying by perhaps 10%.

However, we have also calculated DWR, D_0 and R_{35} for more than ten thousand real crystal size spectra measured in mid-latitude cirrus by the UKMO C-130 aircraft during the EUCREX campaign (see Hogan and Illingworth 1999 for more details), and Fig. 3 shows best-fit relationships derived from them. It can be seen that analytic distributions tend to underestimate the number concentrations of large (millimeter-sized) crystals which are important for determining the radar parameters Z and DWR, but which contribute minimally to D_0. This is probably because there is often some degree of bimodality in real size distributions. We therefore use the empirical relationships derived from the EUCREX data in the the case study that follows. Up to a DWR of 3 dB and D_0 of 700 μm there is not a great deal of difference between the two approaches.

It should be noted that there are a number of ways of defining D_0 that can result in rather different values being derived from a given aircraft-measured size spectrum. Hogan and Illingworth (1999) calculated D_0 simply as the median diameter of the volume-weighted size distribution, but in this paper we use the 'method of moments' (e.g. Kozu and Nakamura 1991) in which the parameters N_0, D_0 and μ in (2) are determined such that three chosen moments of the distribution are conserved. Somewhat different values of D_0 can be derived depending on which moments one chooses to conserve, but here we conserve the zeroth, first and third moments. Using this definition, it is found that 25% of the EUCREX data have a value for D_0 of less than 200 μm, and the same proportion have a value of more than 600 μm.

It has been suggested (e.g. Arnott et al. 1994) that there exist high concentrations of crystals smaller than 50 μm that are not represented in analytic, monomodal approximations for the size distribution. Crystals smaller than 25 μm are also not detected by standard airborne 2D imaging probes, such as those that were mounted on the C-130 aircraft during EUCREX. If present, these crystals could dominate the radiative properties of cirrus clouds while being effectively undetected by radar, therefore invalidating the use of radars to infer radiative properties. However some recent studies have measured down to 5–10 μm using replicators (Mitchell et al. 1996), balloon-borne videosondes (Kinne et al. 1997), and a video ice particle sampler (McFarquhar and Heymsfield 1997), and all suggest that small crystals make a minor contribution to IWC and optical depth. This implies that it is reasonable to use the EUCREX data in this study despite the fact that crystals smaller than 25 μm were not detected.

d. Calibration

Naturally any gains in the accuracy of IWC derived from dual- rather than single-wavelength radar are lost if the radars are not accurately calibrated, both relative to each other and in an absolute sense. The approach here has been to calibrate the 35 GHz radar by comparison with the 3 GHz radar at Chilbolton in light, Rayleigh-scattering rain. This radar in turn has been calibrated in heavy rain to better than 0.5 dB from the consistency of differential reflectivity and differential phase measurements (Goddard et al. 1994). The 94 GHz radar is then calibrated on a case study basis by matching with the reflectivity at 35 GHz in the Rayleigh-scattering cirrus cloud tops. The small correction for attenuation by atmospheric gases is made using the line-by-line model for millimeter-wave propagation of Liebe (1985) coupled with the thermodynamic variables diagnosed by the UKMO Unified Model. Attenuation by the ice crystals themselves is negligible at these frequencies.

3. 22 June 1996 Case Study

On 22 June 1996, vertically-pointing radar reflectivity measurements were made through a thick cirrus cloud by the two cloud radars at Chilbolton. The cloud was associated with a strong jet stream that peaked at 40 m s^{-1} at 9 km over the site. Both radars are of the conventional pulsed type and have pulse lengths of 45 and 75 m at 35 and 94 GHz respectively (although both were sampled every 75 m). The beamwidth of the 35 GHz radar is 0.4° and that of the 94 GHz radar is 0.5°, and they were located next to each other on the ground. Gaseous attenuation was corrected for using the methodology outlined in the previous section, and the two-way differential attenuation through the depth of the cloud (5 to 10 km) was found to amount to only 0.1 dB, although the total two-way gaseous attenuation from the ground to 10 km at 94 GHz was 2 dB. Liquid water in the stratocumulus layer beneath would also have attenuated the 94 GHz signal somewhat, but this could not have affected the results because of the way this radar is calibrated. A vertically-pointing lidar ceilometer was also in operation on this day but it was found that throughout the period the cirrus was overhead, the lidar signal was completely blocked by the low-level cloud; cloud base was measured as 2.1 km, and the signal was lost by 2.3 km.

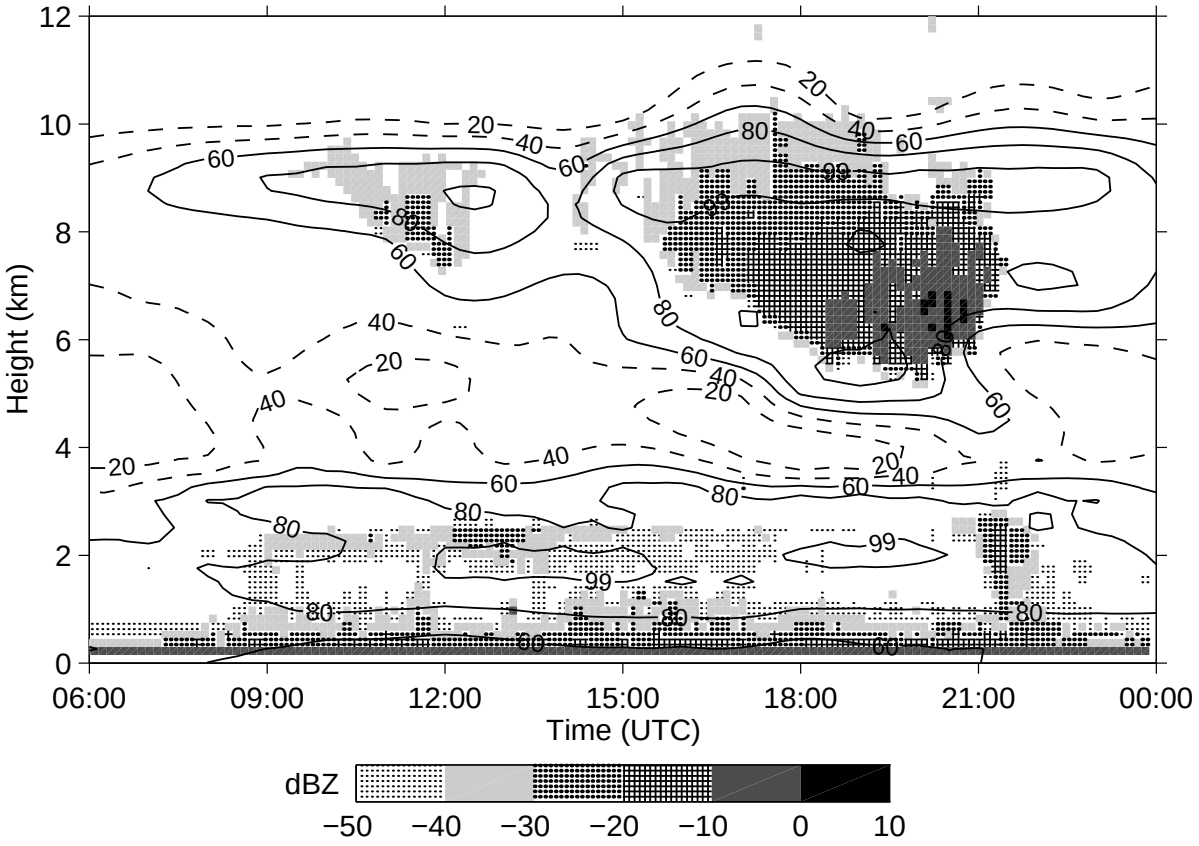

FIG. 4: 35 GHz reflectivity factor with UKMO Unified Model relative humidity contours (%) superimposed, for part of 22 June 1996.

Figure 4 shows a time series of relative humidity from the three-hourly analyses and the T+1 and T+2 forecasts of the model, superimposed on the 35 GHz reflectivity factor. Model parameters over Chilbolton were calculated simply by interpolating linearly between the four nearest model gridpoints at each model level. Relative humidity is taken to be with respect to ice when the temperature is below 0°C. The raw radar data were recorded as 10 second averages with a range-gate spacing of 75 m, but in this figure have been averaged over 8 minutes and 150 meters, enabling a 9.9 dB increase in sensitivity. There is broad agreement between the location of the cloud as indicated by the radar, and the most humid areas of the model. The sharp observed cirrus cloud base can be explained by the very dry layer beneath the cloud, although the model appears to have positioned both around a kilometer too low. Note that both insects and ground-clutter are apparent in the radar data below 1 km.

Figure 5 shows dual-wavelength measurements together with derived IWC and D_0 for a shorter period of the day, calculated using the relationships derived from the EUCREX dataset and the density function given by (4). The data have been averaged over 2 minutes and 150 m. Also shown is IWC as diagnosed by the model, with model datapoints indicated by black dots, and a comparison between the ice water path (IWP) measured by the model and the radars.

Size measurements are not possible in the upper parts of the cloud where DWR is only slightly greater than 0 dB. To determine how low DWR can get before sizing is impossible, we need to know the errors in reflectivity and hence in DWR. It can be shown that for a radar with a noise-equivalent reflectivity (for a single pulse) N, the standard error of a reflectivity measurement averaged over M_I independent pulses is given by

$$\Delta Z \simeq \frac{4.343}{\sqrt{M_\mathrm{I}}} \left(1 + 10^{0.1(N[\mathrm{dBZ}] - Z[\mathrm{dBZ}])}\right) \ \mathrm{dB}. \qquad (6)$$

At a range of 1 km, $N = -34$ dBZ at 35 GHz and $N = -23$ dBZ at 94 GHz. The pulse repetition frequencies were 3125 and 5000 Hz at 35 and 94 GHz respectively, although only every fifth pulse at 94 GHz and every tenth

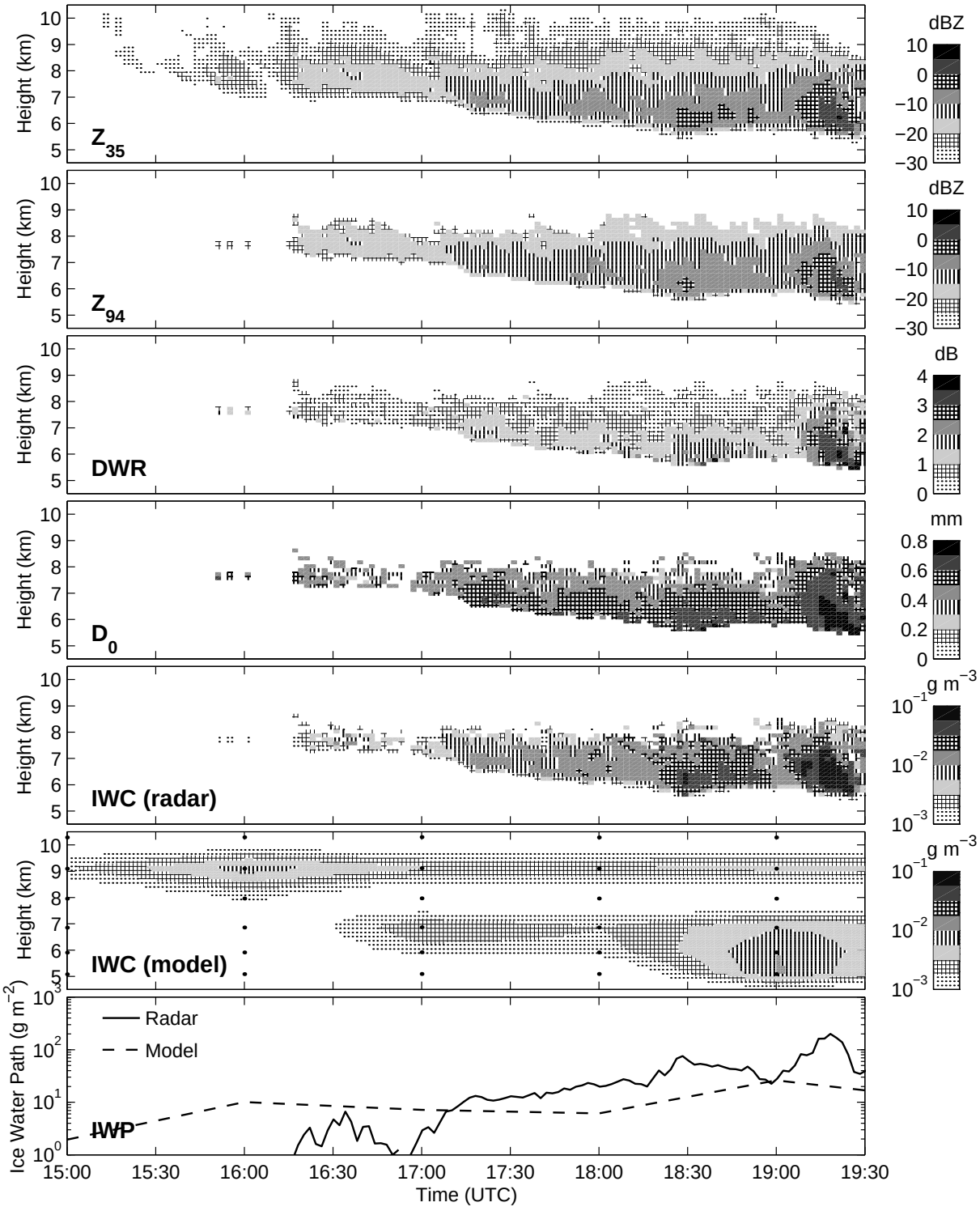

FIG. 5: Time-series of dual-wavelength radar data and derived quantities obtained on 22 June 1996: (from top) 35 GHz reflectivity factor; 94 GHz reflectivity factor; dual-wavelength ratio; median volume diameter; ice water content derived from radar; ice water content diagnosed by the UKMO Unified Model (where the black dots indicate the model gridpoints); ice water path from the model and the radar.

pulse at 35 GHz were used in the real-time averaging. The data of Fig. 5 are presented in Fig. 6 as a scatterplot of Z_{35} against DWR, with lines of constant IWC superimposed. The error bars represent the accuracy achievable assuming all pulses are independent, although the scatter of the data at low reflectivity (where DWR should be close to 0 dB) appears to be somewhat more than that indicated by the length of the error bars. However, exact calculation of M_{I} requires the spectral width, a parameter that was not measured during this case study.

We follow the suggestion of Matrosov (1993) and calibrate DWR by matching Z_{35} and Z_{94} at cloud top, but it is clear that the scatter of the data at low reflectivity is such that this cannot be done to a high degree of accuracy. The problem stems from the fact that the 94 GHz radar was around 10 dB less sensitive than the 35 GHz when these data were taken, thus introducing large errors in DWR when measuring close to its sensitivity limit. This was due to a technical problem that has since been rectified. We have imposed the condition that for an observation to be used, DWR must be larger than twice the standard error in DWR. This threshold at an altitude of 7 km is illustrated by the dashed line in Fig. 6 and all points below this are rejected for the purposes of size and IWC measurement.

The cloud-free layer in the model at around 8 km was not observed in the radar data, and is due to the workings of the large-scale cloud and precipitation schemes, in which IWC is calculated every timestep simply as the total water content (a prognostic variable) minus the saturation vapor density, with an allowance for humidity fluctuations over the gridbox (UKMO, personal communication). The timestep for the Mesoscale Version of the model is 5 minutes. An excess of ice is precipitated out instantaneously, so that ice water cannot persist in regions where the relative humidity is below a certain critical value, even if it is falling from a saturated layer above. In this case the model relative humidity fell to around 85%. In fact between 9 and 9.5 km the horizontally-averaged 35 GHz reflectivity exhibited an increase with height of about 2 dB in an otherwise monotonically decreasing profile, indicating that a little evaporation was occuring. These observations illustrate a shortcoming in the model that may have an impact on radiative properties.

For radiative calculations the model prescribes an effective radius of 30 μm, but unfortunately the calculation of this parameter from radar-derived D_0 is particularly sensitive to the assumed crystal density, and our confidence in density is not sufficient to attempt any comparison with the model value. Radar-retrieved values of D_0 are however more than an order of magnitude greater than this value.

We next examined the profile of radar and microphysical properties along individual fallstreaks. Figure 7 shows part of the 35 GHz reflectivity data at the highest available resolution of 75 meters and 10 seconds, together with the trajectories of three fallstreaks. These were derived by first finding the times of the maxima in Z_{35} at each rangegate. A point near cloud top was selected, and then the nearest maximum at the next height down was chosen. This process was repeated through the depth of the cloud, and finally a fifth-order polynomial was fitted through the selected points. In Fig. 8 the corresponding plots of DWR against Z_{35}, and D_0 against IWC have been plotted. It can be seen that in the evaporating region at cloud base the crystals tend to be larger for a given IWC compared with those in the bulk of the cloud. This is consistent with the idea that the smallest crystals evaporate first.

4. Conclusions

The potential of dual-wavelength radar for remote measurement of crystal size, and hence of ice water content, has been demonstrated. Scattering calculations suggest that variations in density from cloud to cloud may somewhat bias the results, although this would also be true of single-wavelength estimates of IWC. A discrepancy between the crystal densities implied by Brown and Francis (1995) and Francis et al. (1998) has been found, and it is not obvious which is the most appropriate to use for radar. There is also the problem that both were calculated to maximize the agreement between two independent measurements of IWC, so are not necessarily valid for millimeter-sized crystals that can contribute significantly to Z but very little to IWC. It is very important that the issue of density is resolved, because of the implications for this remote sensing technique and others, and also in order that the dual-wavelength method can be extended to making estimates of effective radius. Evidence has been presented to suggest that operating the radars at an elevation of 45° should greatly reduce the errors introduced by approximating all crystals as spheres, thereby eliminating the need for a priori knowledge of the predominant crystal habit in the cloud.

Dual–wavelength observations of a real cirrus cloud have measured median volume diameters of up to 0.8 mm, and a distinct difference in the crystal size at the base and top of the cloud for a given IWC was observed. It is evident that for useful, quantitative radar measurements in cirrus clouds, the instruments themselves must be both well calibrated and very sensitive. In this study DWR was observed to approach 0 dB for reflectivity factors below around -20 dBZ. Even with considerable averaging the 94 GHz radar had a minimum detectable reflectivity of only around -25 dBZ at cirrus altitudes, so random scatter of the data at these low signal-to-noise ratios made precise matching of the two radars in the Rayleigh-scattering cloud top difficult. It also meant that median diameters of less than around 200 μm could not be measured, although in future with both radars sensitive down to -35 dBZ it should be possible to measure diameters of 100 μm.

In this very limited comparison the UKMO model was

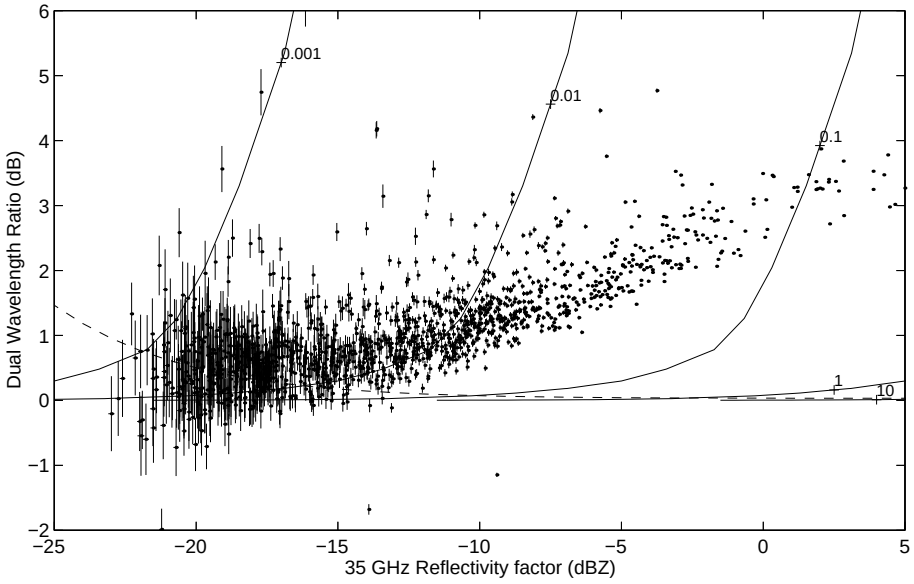

FIG. 6: Scatterplot of Z_{35} versus DWR for the data presented in Fig. 5 with lines of constant IWC (labelled in g m^{-3}) overlayed. The error bars have been calculated assuming all pulses are independent, and the dashed line indicates the threshold for the rejection of data for the purposes of size retrieval, at an altitude of 7 km.

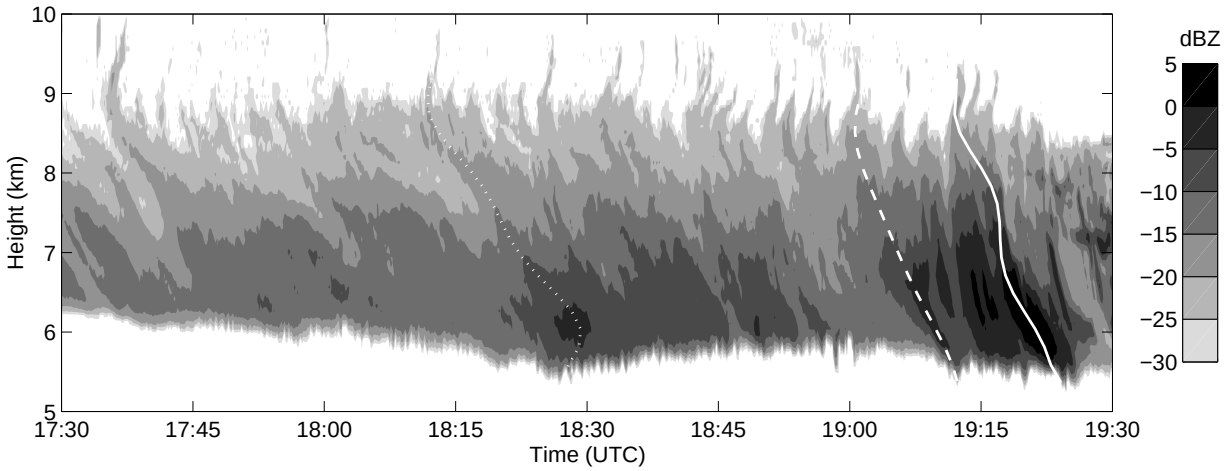

FIG. 7: High resolution 35 GHz reflectivity factor with objectively-derived fallstreaks overlayed.

found to perform reasonably well in locating the cirrus cloud, although the nature of the large-scale cloud scheme in the model is such that there is a direct dependence of IWC on relative humidity. This meant that layers of cirrus were formed in coincidence with saturated and sub-saturated layers when in reality the crystals fell an appreciable distance through the sub-saturated air, with only a slightly detectable decrease in reflectivity due to evaporation. Cloud radar clearly has a role to play in model validation, although for an objective assessment of model performance at least a month-long dataset of radar observations would be required. Before this can happen it is essential that the dual-wavelength technique is itself validated, by comparing retrieved size and IWC with simultaneous in situ measurements by aircraft.

The use of 94 GHz as the shorter wavelength is necessary for ground-based observations to keep gaseous attenuation down to an acceptable level, but since median volume diameter rarely exceeds 1 mm, the magnitude of the dual-wavelength ratio is generally less than 4 dB. Furthermore, the mean crystal size in a significant fraction of cirrus clouds is too low for the technique to work. From space however higher frequencies become viable, which has a number of advantages, the most pertinent for a dual-

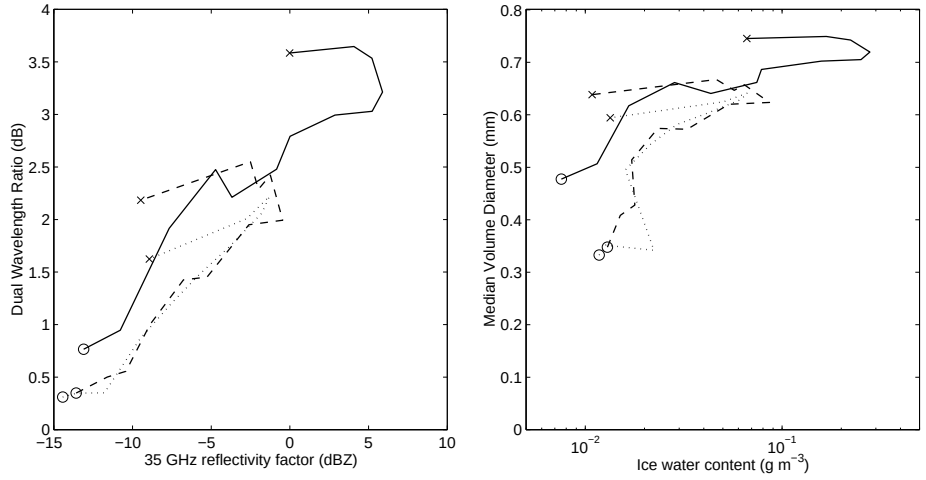

FIG. 8: DWR against Z_{35}, and D_0 against IWC for the three fallstreaks highlighted in Fig. 7, using the same line-styles. The circles indicate the top of the streaks and the crosses indicate the bottom.

wavelength system being larger (and hence more measurable) values of DWR, which in turn enables more accurate size measurement and a lower minimum measurable size (Hogan and Illingworth 1999).

Acknowledgements

We are grateful to the Radio Communications Research Unit at the Rutherford Appleton Laboratory for the use of the Chilbolton radars, to Drs. Ed Dicks and Peter Panagi for providing the model data, and to Philip Brown for supplying the EUCREX data. The T-matrix code was written and provided by S. Vivekanandan. Invaluable support for the 94 GHz radar has been provided by ESTEC (contract 10568/93). This research also received funding from NERC (grant GR3/8765), and the first author was supported by a NERC studentship.

REFERENCES

Arnott, W. P., Y. Y. Dong and J. Hallett, 1994: Role of small ice-crystals in radiative properties of cirrus: A case study, Fire II 22 Nov 1991. *J. Geophys. Res.*, **99**, 1371–1381.

Atlas, D., and F. H. Ludlam, 1961: Multi-wavelength radar reflectivity of hailstorms. *Quart. J. Roy. Meteor. Soc.*, **87**, 523–534.

Brown, P. R. A., and P. N. Francis, 1995: Improved measurements of the ice water content in cirrus using a total-water probe. *J. Atmos. Oceanic Technol.*, **12**(2), 410–414.

Brown, P. R. A., A. J. Illingworth, A. J. Heymsfield, G. M. McFarquhar, K. A. Browning and M. Gosset, 1995: The role of spaceborne millimeter-wave radar in the global monitoring of ice-cloud. *J. Appl. Meteor.*, **34**(11), 2346–2366.

Francis, P. N., P. Hignett and A. Macke, 1998: The retrieval of cirrus cloud properties from aircraft multi-spectral reflectance measurements during EUCREX '93. *Quart. J. Roy. Meteor. Soc.*, **124**, 1273–1291.

Goddard, J. W. F., J. Tan and M. Thurai, 1994: Technique for calibration of meteorological radars using differential phase. *Electronics Letters*, **30**(2), 166–167.

Herman, G. F., and J. A. Curry, 1984: Observational and theoretical studies of solar radiation in arctic stratus clouds. *J. Climate Appl. Meteor.*, **23**, 5–24.

Heymsfield, A. J., L. M. Miloshevich, A. Slingo, K. Sassen and D. O'C. Starr, 1991: An observational and theoretical study of highly supercooled altocumulus. *J. Atmos. Sci.*, **48**(7), 923–945.

Hogan, R. J., and A. J. Illingworth, 1999: The potential of spaceborne dual-wavelength radar to make global measurements of cirrus clouds. *J. Atmos. Oceanic Technol.*, **16**(5), 518–531.

Intrieri, J. M., G. L. Stephens, W. L. Eberhart and T. Uttal, 1993: A method for determining cirrus cloud particle sizes using lidar and radar backscatter techniques. *J. Appl. Meteor.*, **32**(6), 1074–1082.

Kinne, S., T. P. Ackerman, M. Shiobara, A. Uchiyama, A. J. Heymsfield, L. Miloshevich, J. Wendell, E. W. Eloranta, C. Purgold and R. W. Bergstrom, 1997: Cirrus cloud radiative and microphysical properties from ground observations and in situ measurements during FIRE 1991 and their application to exhibit problems in cirrus solar radiative transfer modeling. *J. Atmos. Sci.*, **54**, 2320–2344.

Kosarev, A. L., and I. P. Mazin, 1989: Empirical model of physical structure of the upper level clouds of the middle latitudes. *Radiation Properties of Cirrus Clouds.* Nauka, 29–52.

Kozu, T. and K. Nakamura, 1991: Rainfall parameter estimation from dual-radar measurements combining reflectivity profile and path-integrated attenuation. *J. Atmos. Oceanic Technol.*, **8**, 259–270.

Liebe, H. J., 1985: An updated model for millimeter-wave propagation in moist air. *Radio Science,* **20**(5), 1069–1089.

Liebe, H. J., T. Manabe and G. A. Hufford, 1989: Millimeter-wave attenuation and delay rates due to fog/cloud conditions. *IEEE AP,* **37**, 1617–1623.

Liou, K.-N., 1986: Influence of cirrus clouds on weather and climate processes: A global perspective. *Monthly Weather Rev.*, **114**, 1167–1199.

Martin, G. M., D. W. Johnson and A. Spice, 1994: The measurement and parameterization of effective radius of droplets in warm stratocumulus clouds. *J. Atmos. Sci.*, **51**(13), 1823–1842.

Matrosov, S. Y., 1993: Possibilities of cirrus particle sizing from dual-frequency radar measurements. *J. Geophys. Res.*, **98**(D11), 20 675–20 683.

Matrosov, S. Y., B. W. Orr, R. A. Kropfli and J. B. Snider, 1994: Retrieval of vertical profiles of cirrus cloud microphysical parameters from Doppler radar and infrared radiometer measurements. *J. Appl.*

Meteor., **33**, 617–626.

Maxwell-Garnet, J. C., 1904: Colours in metal glasses and metallic films. *Philos. Trans. Roy. Soc.,* **A203**, 385–420.

McFarquhar, G. M., and A. J. Heymsfield, 1997: Parameterization of tropical cirrus ice crystal size distributions and implications for radiative transfer: Results from CEPEX. *J. Atmos. Sci.,* **54**, 2187–2200.

Mitchell, D. L., S. K. Chai, Y. Liu, A. J. Heymsfield and Y. Dong, 1996: Modeling cirrus clouds. 1: Treatment of bimodal size spectra and case study analysis. *J. Atmos. Sci.,* **53**(20), 2952–2966.

O'Brien, S. G., and G. H. Goedecke, 1988: Scattering of millimeter waves by snow crystals and equivalent homogeneous symmetric particles. *Appl. Optics,* **27**(12), 2439–2444.

Rinehart, R. E., and J. D. Tuttle, 1982: Antenna beam patterns and dual-wavelength processing. *J. Appl. Meteor.,* **21**, 1865–1880.

Sassen, K., 1991: Aircraft-produced ice particles in a highly supercooled altocumulus cloud. *J. Appl. Meteor.,* **30**(6), 765–775.

Schneider, T. L., and G. L. Stephens, 1995: Theoretical aspects of modeling backscattering by cirrus ice particles at millimeter wavelengths. *J. Atmos. Sci.,* **52**(23), 4367–4385.

Sekelsky S. M., W. L. Ecklund, J. M. Firda, K. S. Gage and R. E. McIntosh, 1999: Particle size estimation in ice-phase clouds using multifrequency radar reflectivity measurements at 95, 33 and 2.8 GHz. *J. Appl. Meteor.,* **38**(1), 5–28.

Stephens, G. L., S. C. Tsay, P. W. Stackhouse Jr. and P. J. Flatau, 1990: The relevance of the microphysical and radiative properties of cirrus clouds to climate and climatic feedback. *J. Atmos. Sci.,* **47**, 1742–1752.

Tuttle, J. D., and R. E. Rinehart, 1983: Attenuation correction in dual-wavelength analyses. *J. Climate Appl. Meteor.,* **22**, 1914–1921.

Waterman, P., 1969: Scattering by dielectric obstacles. *Alta Freq.,* **38**, 348–352.